Obrabotka metallov -
Metal Working and Material Science

Journal homepage: http://journals.nstu.ru/obrabotka_metallov

Thermomechanical rolling in well casing production (research review)

Kirill Baraboshkin [1, a], **Ruslan Adigamov** [1, b], **Vladimir Yusupov** [2, c], **Irina Kozhevnikova** [3, d], **Antonina Karlina** [1, e, *]

[1] JSC "Severstal Management", 30 Mira str., Cherepovets, 162608, Russian Federation

[2] Baikov Institute of Metallurgy and Materials Science, RAS, 49 Leninsky Prospekt, Moscow, 119334, Russian Federation

[3] Cherepovets State University, 5 Lunacharsky pr., Cherepovets, Vologda region, 162600, Russian Federation

[a] https://orcid.org/0009-0004-9054-3523, ka.baraboshkin@severstal.com; [b] https://orcid.org/0009-0006-7620-5872, rradigamov@severstal.com;
[c] https://orcid.org/0000-0002-0640-2217, vsyusupov@mail.ru; [d] https://orcid.org/0000-0003-0810-2143, iakozhevnikova@chsu.ru;
[e] https://orcid.org/0000-0003-3287-3298, ai.karlina@severstal.com

ARTICLE INFO

ABSTRACT

Introduction. The modern oil and gas industry requires the development of high strength materials for well casing. Changes in rolled steel production technologies are one of the urgent tasks. Reducing the cost of high quality steel well casing is becoming a major challenge for the oil and gas industry. Multiphase microstructures containing acicular ferrite or an acicular ferrite-dominated phase exhibit good complex properties in *HSLA* steels. This paper focuses on the results obtained using modern methods of thermomechanical rolling. **Results and discussion.** This work analyzes the characteristics of thermomechanical rolling technologies and its impact on the microstructure of rolled steel for well casing. It is shown that predicting mechanical properties based on the microstructural characteristics of steel is complicated due to the large number of parameters involved. This requires an optimal microstructure of the steel. A satisfactory microstructure depends on several factors, such as chemical composition, hot work processing, and accelerated cooling. Alloying elements have a complex effect on the properties of steel, and alloying additives are usually introduced into the steel composition. From a metallurgical point of view, the choice of alloying elements and the metallurgical process can greatly influence the resulting microstructure. **Conclusion.** This review reports the most representative study regarding thermomechanical rolling technologies and microstructural factors in well casing steels. It includes a summary of the most important process variables, material properties, regulatory guidelines, and microstructural and mechanical properties of the metal for well casing production. This review is intended to benefit readers from a variety of backgrounds, from non-metal forming or materials scientists to various industrial application specialists and researchers.

Introduction

Currently, drilling companies have begun to experiment with new type of pipes, called "casing pipes", for drilling wells [1–12]. The reason for this conversion is that the latter option provides better drilling efficiency than previous generation solutions and has many other advantages [13–21]. The casing pipe lowered from the surface for fixing the walls of the borehole is shown in Figure 1.

The process of rotary drilling with a column and extraction of a hydraulically expandable bit [22–29] reduces drilling efficiency and increases the unproductive time (*UPT*) of this highly capital-intensive industry, stimulating the development of the oil industry to look for new technologies. *Casing Drilling*, or *Casing*

***** Corresponding author**
Karlina Antonina I., Ph.D. (Engineering), Leading Expert
JSC "Severstal Management",
30 Mira str.,
162608, Cherepovets, Russian Federation
Tel: +7 950 120-19-50, **e-mail:** ai.karlina@severstal.com

Main elements of the well

1 — hole mouth;
2 — hole walls;
3 — face of hole;
4 — wall sections secured with casing pipes;
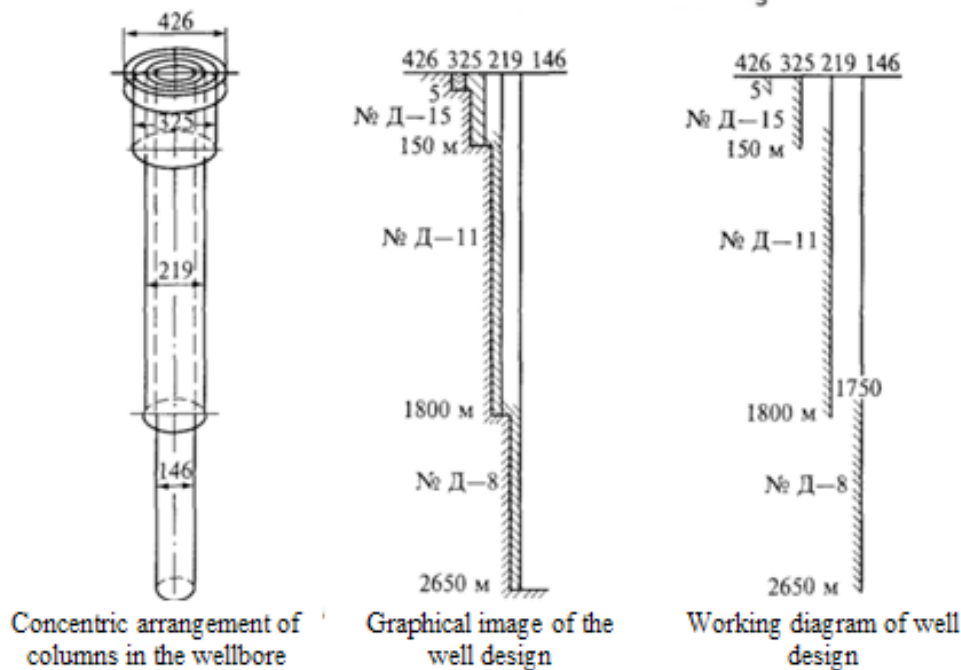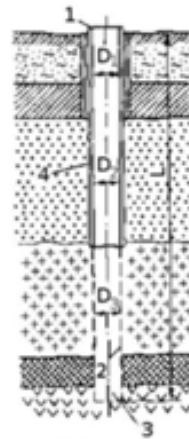D_1, D_2, D_3 — diameters of casing pipes and wellbore;
L — well depth.

Concentric arrangement of columns in the wellbore

Graphical image of the well design

Working diagram of well design

Fig. 1. Well casing design

while Drilling (*CwD*) is a drilling method that has been proven to eliminate many problems encountered during drilling. In this method, drilling and casing of the borehole are carried out simultaneously, which increases drilling efficiency by reducing the *UPT* [1–5, 30–36].

Russian oil companies reported the use of retractable bits in casing drilling in 1920. Later, in the 1930s, USA operators used operational tubing for drilling in an open shaft or finishing without a face, while a flat-bladed chisel was used for drilling [37–42]. The materials that best meet the requirements of the oil and gas industry are *HSLA* steels.

The purpose of the work is to assess the influence of thermomechanical processing technologies on the microstructure and mechanical properties of high-strength steels based on the analysis of various studies conducted by various methods of metallography and mechanical properties tests, taking into account the influence of recrystallization, microstructural components and microphases. The objective of this analysis is to establish the relationship between microstructure and thermomechanical processing technologies in the production of casing pipes.

The objectives of the work are to study the effect of *Nb* in industrial steels and identify the most effective methods for determining it at a low percentage, as well as to study various thermomechanical controlled rolling *(TMCR)* models and its effectiveness.

Research results of various authors and discussion

Chemical composition of microalloyed steels

In 1936, it was discovered that microalloying additions of metal niobium could strengthen "soft" steels, although the main strengthening mechanism could not be identified at that time.

Steels containing a small amount of vanadium or titanium have been available for a long time, the rapid development and use of microalloyed steels was initiated by the recognition of the advantages of adding a small amount of niobium in *C-Mn* steels [13–21]. This happened in 1958 with the first successful production of niobium-treated steel by *Great Lakes Steel Corporation* in the USA [22–28, 46]. Various factors contributed to this development, including the relatively affordable availability of ferroniobium in the late 1950s and the discovery of very large deposits of ores containing niobium in Brazil and Canada at that time, which guaranteed the stability of future supplies and prices. The advantage of grain refinement effects due to the release of microalloyed elements in the presence of *N* and *C* was well known [13–16, 29–39, 46].

Steels used up to 1980 are characterized by the use of air cooling of the sheet and high strip winding temperatures. As already noted [1–3, 43–46], these are steels with a ferrite-pearlite structure with a strength of up to ~420 MPa. The most obvious factor affecting strength was grain refinement.

The release of carbides and nitrides occurs at 3 stages of processing of micro-alloyed steels. *Type 1* particles are formed in the liquid phase and during or after solidification at the liquid/solid interface and in **δ**-ferrite [14]. *Type 2* particles are deposited in austenite during hot deformation, such as controlled rolling, as the temperature decreases [14]. *Type 3* particles are formed during or after the phase transformation of austenite into ferrite, originating at the austenite/ferrite interface and in ferrite [13–17]. Electron microscope image of the films (Figure 2) showed that these particles, with sizes up to 150 nm, are mainly located in the form of ribbons along the boundaries of austenitic grains or in former inter-dendritic regions [47–48].

In [49], various methods were used to track the release of microalloys after modeling various conditions of thermomechanical controlled rolling (*TMCR*) of austenite in the *Gleeble* thermomechanical simulator. Atom probe tomography (*APT*), scanning transmission electron microscopy using focused ion beam (*STEM-on-FIB*), and electrical resistivity measurements provided additional information about the state of the particles and were correlated with each other. It has been demonstrated that accurate measurements
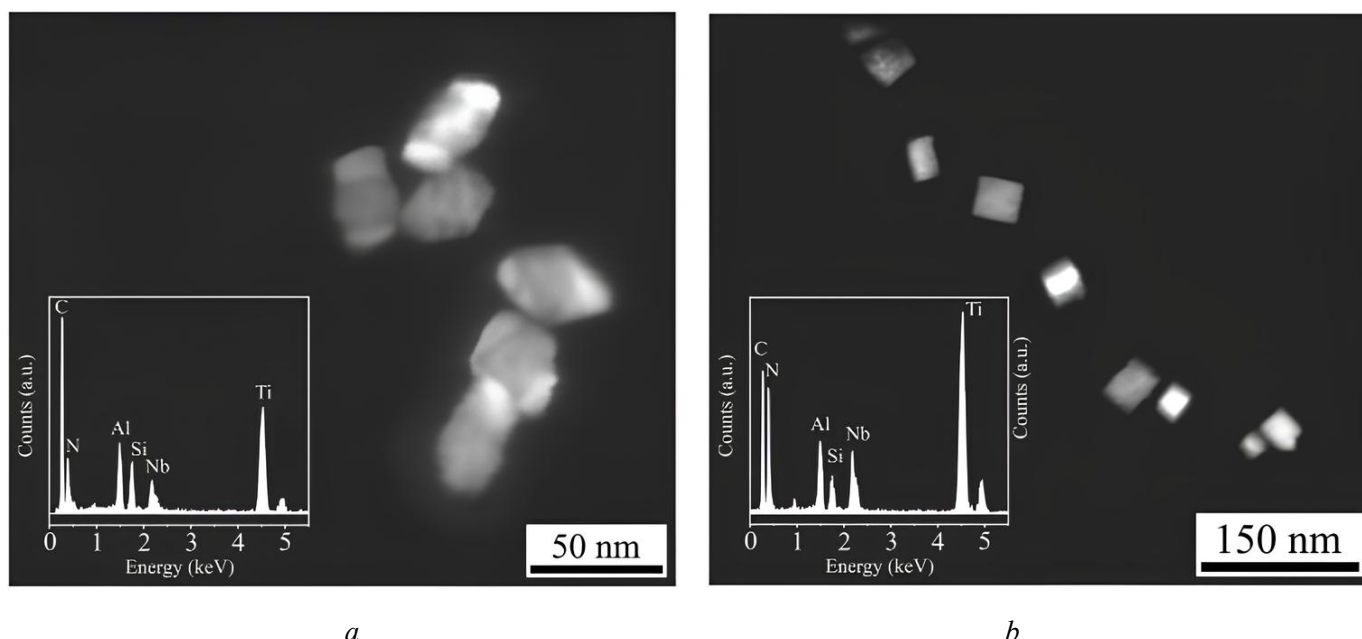

a   *b*

Fig. 2. TEM micrographs of extraction of predominantly *TiN* particles:
a – probably particles formed during solidification; *b* – particles of *NbC* grown on the *TiN* core [48]

of electrical resistivity in steel can control the total consumption of dissolved microalloys (*Nb*) during hot treatment. The obtained results were supplemented with *APT* measurements of the steel matrix. Particles that formed during cooling or isothermal exposure could be distinguished from particles caused by deformation by confirming *STEM* measurements with *APT* results, since *APT* specifically provided detailed information about the chemical composition of particles, as well as the distribution of elements (Figure 3, 4).
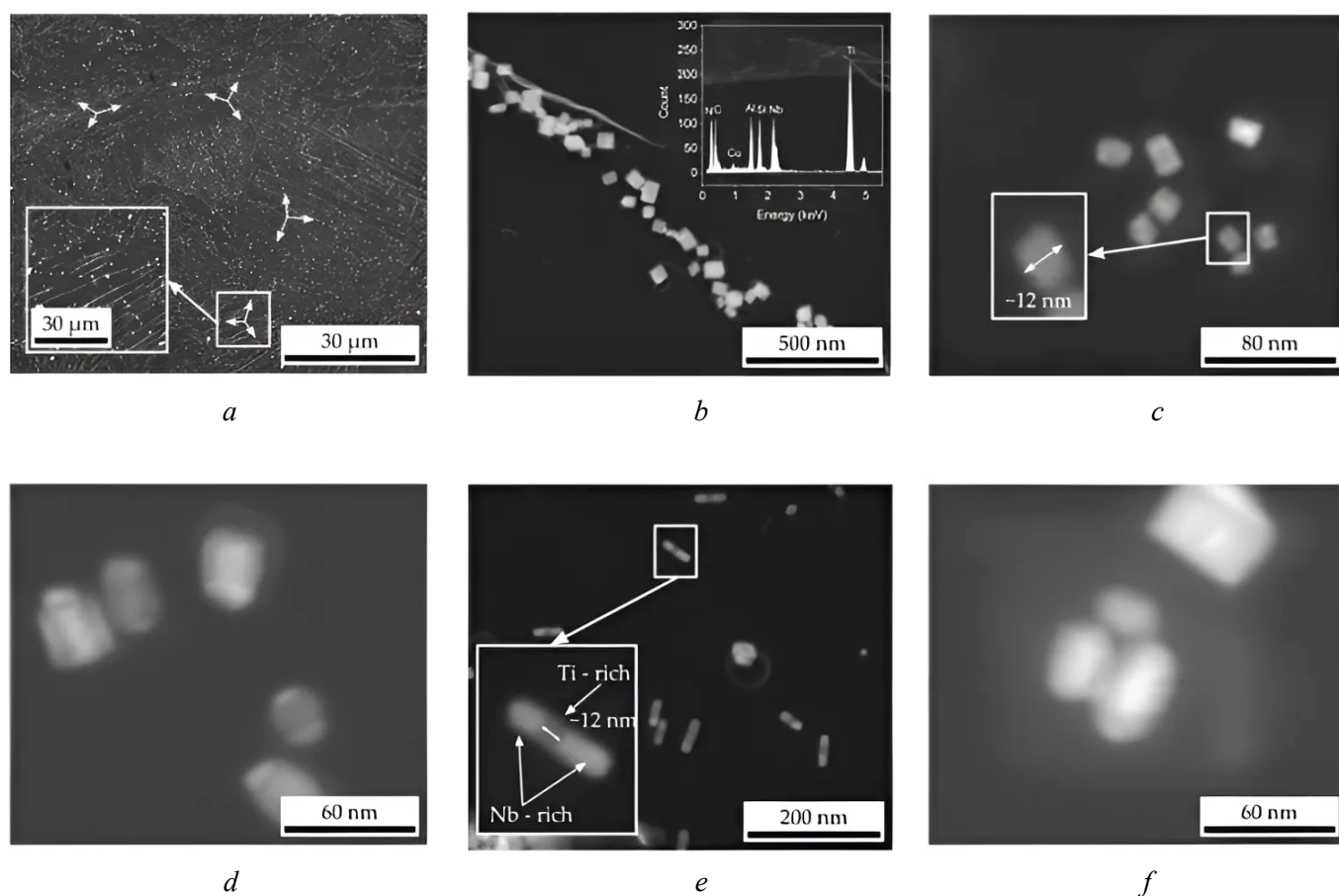

Fig. 3. High-angle diffraction in a dark field (*HADDF*)-*STEM* images containing particles present after quenching from 1,200 °C and 950 °C:

a – grain boundaries with *TiN* particles; *b* – large (approximately 80 nm) cuboid particles, which *EDS* identified as *TiN* enriched with *Nb*; *c* – smaller *TiN* particles (<15 nm); *d* – *TiN* with *Nb* nuclei; *e* – *TiN* with larger *Nb* nuclei are uniformly distributed inside the grain; *f* – particles enriched with *Nb* or *TiNb* (or *Ti*) (*C*, *N*) [49]

Later it was discovered that *Nb* could slow down the recrystallization rate of austenite [48], which was associated with the introduction of controlled rolling and thermomechanical controlled treatment [49, 50]. The effect of the microalloying content (wt. %) on the recrystallization of austenite is shown in Figure 5.

The *C* content used in *HSLA* steels before 1980 was 0.07–0.12 %. Meanwhile, up to 2 % *Mn* content was usually used together with various additives and combinations of *V*, *Nb* and *Ti* (max. 0.1 %) [46, 52–55]. Reducing the *C* content could improve weldability while maintaining strength, and it was the same as that of soft steels, but the main problem with reducing the *C* content was that ductility and toughness were not as good as those of quenched and tempered steels [14]. By adding microalloying elements into the steel composition, the critical temperatures of austenite transformation can be controlled in order to achieve the final mechanical properties [1, 2, 13, 14, 46, 47, 53–55]. These critical temperatures are: the grain coarsening temperature during reheating, the recrystallization temperature during hot rolling, and the transformation temperature during cooling [1, 2, 14, 46, 53, 54]. The main effects of micro-alloying elements are shown in Table [53].
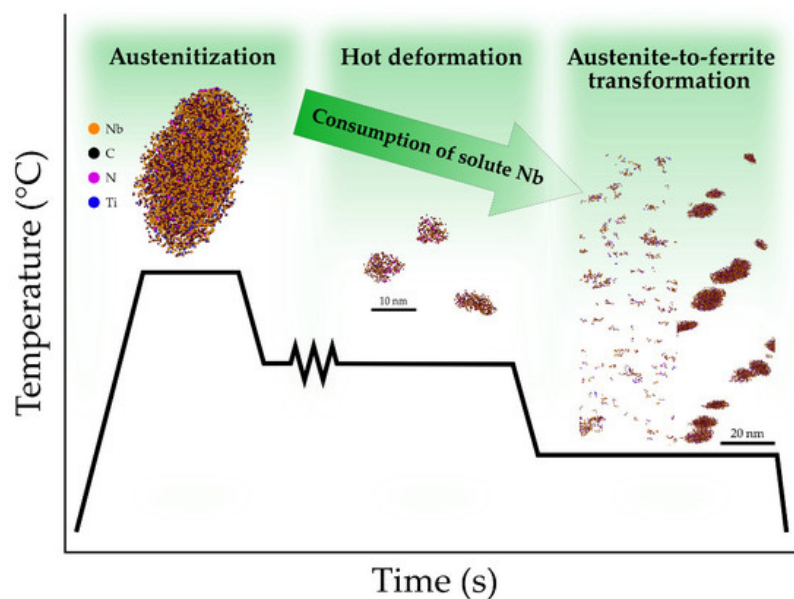
Fig. 4. Kinetics of particle separation in microalloyed *Nb-Ti* steel, as well as the sequence of separation in typical steel during thermomechanical controlled rolling [49]
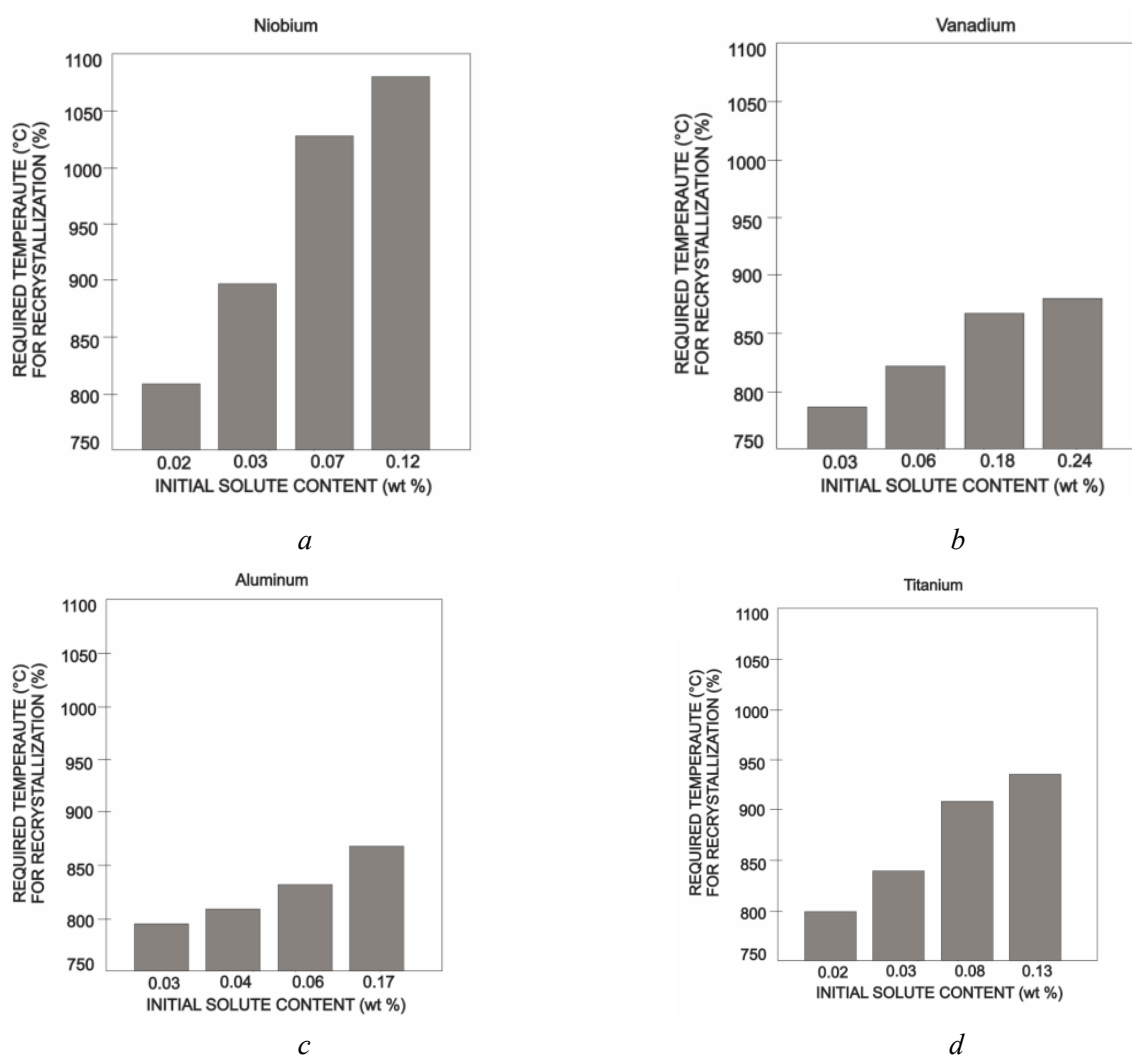

a

b

c

d

Fig. 5. Recrystallization of austenite depending on the content of niobium (*a*), titanium (*b*), aluminum (*c*) and vanadium (*d*) [51]

Operating principle of microalloying elements [53]

Element	wt. %	Effect
C	<0.25	Strengthening
Mn	0.5–2.0	Slows down the decay of austenite during accelerated cooling Reduces the transition temperature from viscous to brittle fracture.
Si	0.1–0.5	Deoxidizer in molten steel. Solid-solution strengthening. Stabilizes austenite
Al	<0.02	Deoxidizer
Nb	0.02–0.06	It strengthens ferrite very strongly in the form of niobium carbides/nitrides
Ti	0–0.06	Austenite grain control by titanium nitrides. Strong ferrite strengthener
V	0–0.10	Strong ferrite strengthener with vanadium carbonitrides
N	<0.012	Detrimental impurity
Mo	0–0.3	Promotes the formation of bainite. Increases the strength of ferrite
Ni	0–0.5	Increases the fracture toughness
Cu	0–0.55	Improves corrosion resistance
Cr	0–1.25	Increases resistance to atmospheric corrosion in the presence of copper
B	0.0005	Increases hardenability
S	<0.05	Detrimental impurity
P	<0.012	Detrimental impurity

Carbon in steel is necessary to obtain the required strength of steel, while strengthening is ensured by the formation of perlite in the steel structure.

Manganese is used to strengthen a solid solution and obtain the required steel strength. It is known that the presence of manganese in steel leads to a shift of $\gamma \rightarrow \alpha$ transformation to a region of lower temperatures, which leads to grain refinement and the formation of ferrite with an increased dislocation density and, as a result, to an increase in the yield strength of steel. To limit the values of the yield strength in rolled products and ensure that the required yield strength values are obtained in the base metal of pipes after pipe processing, as well as to ensure satisfactory weldability, the manganese content is limited to 1.0–1.5 %.

Silicon is used to harden a solid solution and ensure the required strength of steel. Besides, the addition of silicon is necessary for deoxidation of steel during smelting. In accordance with this, the minimum silicon content in steel should be at least 0.15 %. With high silicon content, the number of silicate inclusions increases, which leads to a deterioration in impact strength, thus, the maximum silicon content is limited to 0.80 % to prevent embrittlement of steel.

The addition of aluminum is necessary for deoxidation and modification of steel. At the same time, the minimum sufficient aluminum content is 0.02 %. When the aluminum content is more than 0.06 %, the impact energy decreases.

Chromium, nickel, and copper are added into steel to increase strength properties, as well as to stabilize the structure when heating the metal for rolling and reducing the grain size during rough rolling. In addition, at maximum concentrations of no more than 0.08 %, these elements in steel have a positive effect on the corrosion resistance of pipes.

Titanium in steel is necessary for the binding of nitrogen into *TiN* nitrides, which inhibit grain growth when steel is heated, which contributes to grain grinding.

The nitrogen content in steel is limited to 0.012 %, since the presence of free nitrogen in a solid solution of the α-phase has a negative effect on the operation of the impact during the impact-bending test.

Sulfur and phosphorus are detrimental impurities and its content is limited to values of no more than 0.005 % and no more than 0.012 %, respectively, to ensure high values of impact energy during impact-bending testing.

Vanadium, niobium, and molybdenum are limited by the required mechanical properties.

Calcium is an unavoidable technological impurity. With an increase in the calcium content in the hot-rolled strip, corrosion-active non-metallic inclusions of the first kind are formed, which negatively affects the mechanical properties of rolled products and the corrosion resistance of steel.

The precipitations of *TiN* and *Nb(C,N)* effectively reduce the growth of austenitic grains [14, 46]. *VN*, *NbCN* and *TiC* particles are stable at a normalization temperature of about 900 °C, which creates a sufficient volume fraction of fine particles to control grain growth [56–59]. The *Nb* solid solution and the precipitation of its carbonitrides retard the growth of austenite grains (Fig. 6).
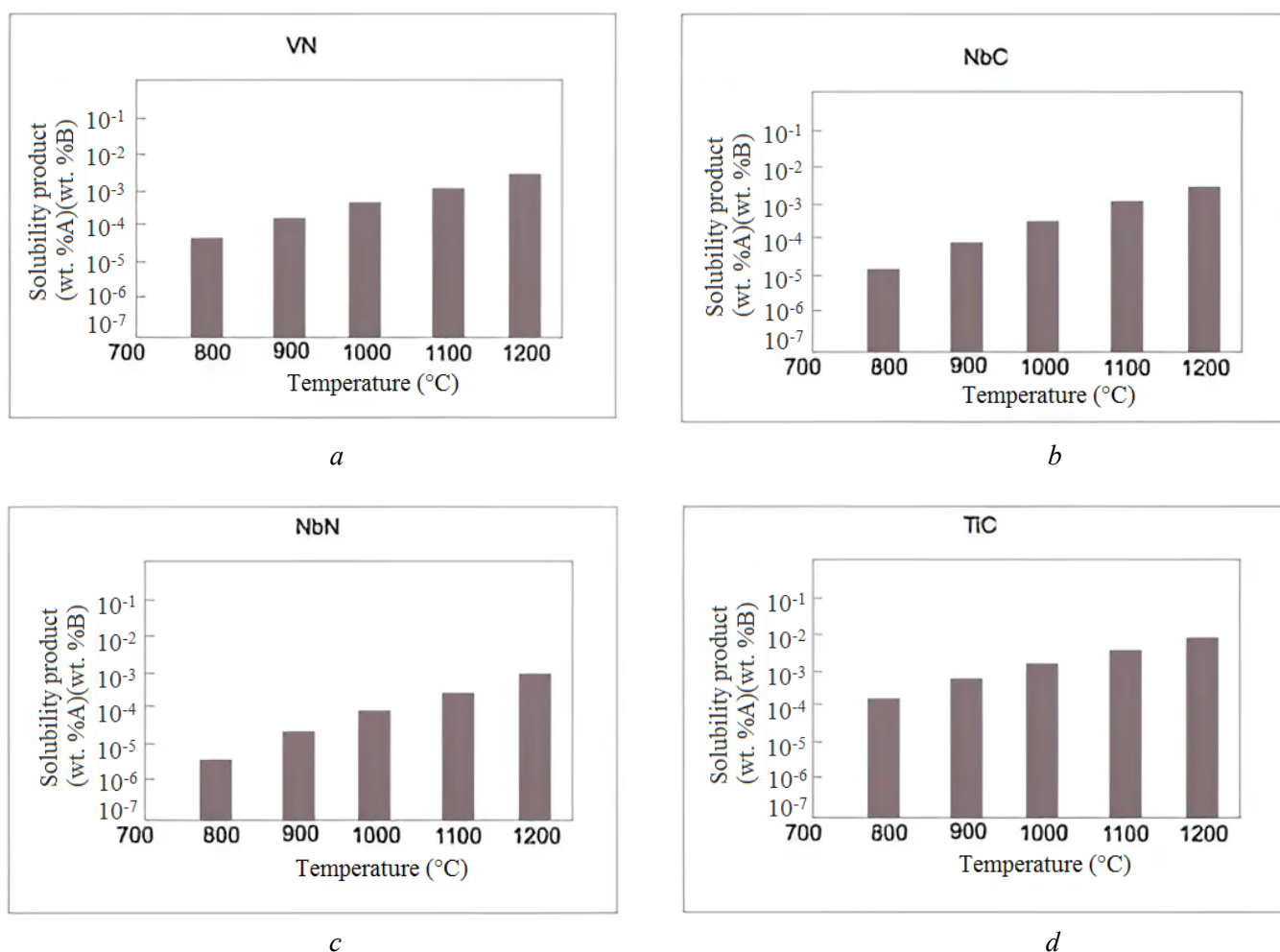
Fig. 6. Solubility of carbonitrides depending on temperature:
a – vanadium nitride; *b* – niobium carbide; *c* – niobium nitride; *d* – titanium carbide [59]

On the other hand, small *Ti* additives cause fine separation of nanoscale carbides, which limits the growth of austenitic grains at higher temperatures (1,200 °C) [15, 16]. *Ti* is released during steel solidification and causes a local concentration that promotes the precipitation of large *TiN* particles [15, 16].

TiC particles can also cause strengthening. Vanadium is the most versatile precipitation strengthening element and is effective in a variety of micro-alloy steel compositions, as well as higher carbon steels. It has been noted in the literature that vanadium carbonitrides *V(C,N)* can potentially create sites for ferrite nucleation. A small lattice mismatch between vanadium nitride (*VN*) (lattice parameters = 0.4139 nm) and ferrite (lattice parameters = 0.2865 nm) promotes ferrite nucleation [14, 45, 46].

The use of controlled cooling reduces the amount of alloying elements required, and steels can reach strengths of about 600 MPa [60–64].

Scientists continue to make efforts to develop high-strength low-alloy (*HSLA*) steels with a combination of high strength and high toughness. To obtain good toughness and weldability, the carbon content is reduced. The decrease in strength due to lower carbon content is compensated by the addition of *Si* and *Mn*. Further increases in strength are achieved through precipitation hardening and grain size reduction by microalloying *Nb*, *V* and *Ti* individually or in combination [65, 66]. It has been established that vanadium atoms in solution delay the bainite reaction at lower transformation temperatures (by 30–40 °C) within the cooling rate range of 1–50 °C/s [64–71].

Nano-sized carbonitrides are formed during prolonged soaking at 450–650 °C, which significantly increases the yield strength, preventing the movement of dislocations. Grain refinement is realized when *TiN* particles fix the austenite grain boundary during heating for rolling, and *Nb* and *NbCN* atoms slow down the recrystallization of deformed austenite [54]. Compared to *Nb-Ti* microalloyed steels, *V-N* steels exhibit grain refinement due to intragranular nucleation of ferrite on *VN* particles, partly due to the similar lattice size of *VN* with ferrite [14, 46]. The introduction of *N* into microalloyed *V* steel stimulates the release of V carbonitrides and increases their volume fraction.

Paper [72] used the *CALculation* of *Phase Diagrams* (*CALPHAD*) approach to study the precipitation of nitrides and carbonitrides in pipe steels in response to new developments in complex chemical compositions and thermomechanical processing of high-strength low-alloy (*HSLA*) steels. This software package is based on minimizing the *Gibbs* free energy of individual phases in an equilibrium state. The calculation results showed that the nitride release temperature in *Ti-Nb* microalloyed steels increased depending on the titanium concentration, while the niobium concentration significantly increased the niobium carbonitride release temperature. Carbonitride particles form at much lower temperatures in low carbon steels (< 0.03 wt. %) than in medium carbon steels (> 0.1 wt. %). This is in good agreement with independent experimental data from the literature, where the growth of austenite grains in steels of similar compositions was studied. Although dissolution and particle growth are controlled by process kinetics, these results proved that thermodynamic calculations can effectively predict the composition and sequence of particle formation in chemically complex systems, allowing for more accurate design of experiments to determine critical temperatures for grain coarsening during reheating, heating recrystallization, rolling, and transformation upon cooling. This can minimize the amount of testing required to obtain optimal chemical compositions and heat treatment procedures where austenite grain growth in steel of similar composition has been studied.

In [73, 74], to study the microsegregation phenomena and behavior of complex particles (*Ti,Nb*)(*C,N*) during continuous casting, a unidirectional solidification setup was used to simulate the crystallization process. In the specimens studied by the authors, a dendritic structure was detected along the direction of solidification. This shows that the addition of titanium, niobium to high strength low alloy (*HSLA*) steel results in unwanted (*Ti,Nb*) (*C,N*) precipitates due to microsegregation. The effect of cooling rate on the formation of (*Ti,Nb*) (*C,N*) was investigated. The composition of large particles was determined using *FE-SEM* with *EDS*. Large particles (*Ti,Nb*) (*C,N*) can be divided into three types based on composition and morphology. As the cooling rate increases, *Ti* (*Ti,Nb*) (*C,N*) particles transform into *Nb* (*Ti,Nb*) (*C,N*) particles.

It is noted in [75] that if small *Nb*(*C,N*) and *NbC* particles containing niobium have a diameter of the order of several nanometers, usually ≤ 50 nm, then large particles containing niobium can have a length from submicron to hundreds of micrometers. The formation mechanism of ≤ 50 nm niobium carbide or carbonitride particles is well known, and its beneficial effects on strength and toughness are well documented. Whereas, large *Nb* particles worsen the characteristics of steel. Despite numerous studies of large particles with a high *Nb* content, no experimental evidence has been proposed for the alleged mechanisms of its formation. Defects associated with large *Nb*-rich particles include cracking of slabs during reheating, failures in tensile tests, hydrogen cracking problems, and increased screening under ultrasonic testing.

The work [54] schematically shows the role of niobium for *HSLA* steels in the process of thermomechanical processing (Figure 7).
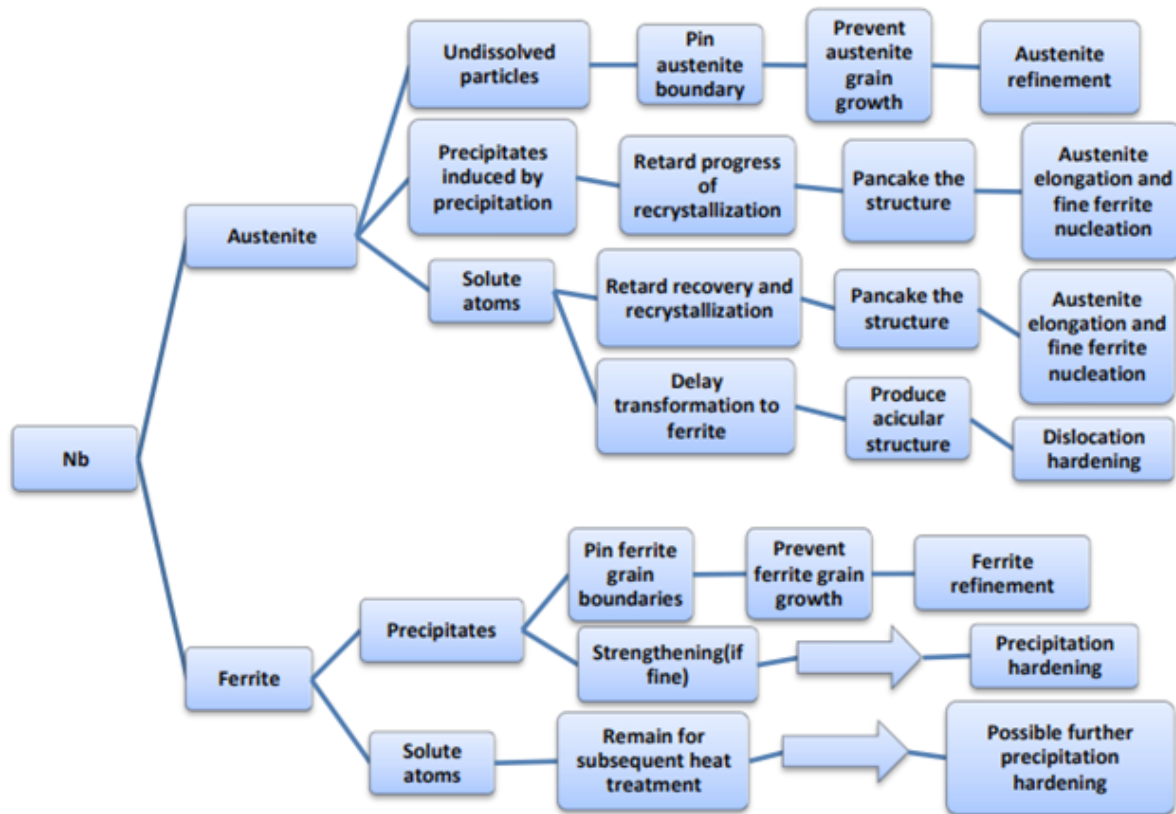
Fig. 7. The role of niobium in *HSLA* steels in the thermomechanical processing process

The above analysis of the literature shows that careful selection of the chemical composition of steel in combination with an appropriate thermomechanical scheme makes it possible to obtain a wide range of microstructures, from classic combinations of ferrite and pearlite to more advanced bainite phases with an optimal balance of mechanical properties.

The accumulation of strain in the austenite is enhanced and consequently the grain sizes in the final microstructures are reduced. The presence of *Mo* promotes the presence of non-polygonal phases, and this constituent modification causes an increase in strength due to the formation of substructure, as well as due to an increase in dislocation density [76–80].

Research in the field of microalloyed steels has expanded over the decades, and the focus has been on improving its strength and environmental resistance through microstructure control.

Advances in desulfurization are important because it helps control microstructure. Over the years, the sulfur content in microalloyed steels has been reduced, allowing the toughness of the steels to continually improve (Figure 8).

Sulfide control is believed to improve the toughness of micro-alloyed steels [77].

In [52], the authors believe that 1980 represents the starting point for the strength of microalloyed steels. From the early 1960s until about 1980, microalloyed steels were low-hardenability steels with a ferrite + pearlite microstructure and a tensile strength ≤ 420 MPa. The obvious choice for solving this problem was the products of low-temperature transformation: matrices consisting of bainite and martensite. This was achieved in the mid-1980s for treating steels using the *Intermittent Accelerated Cooling* (*IAC*) and *Intermittent Direct Quenching*
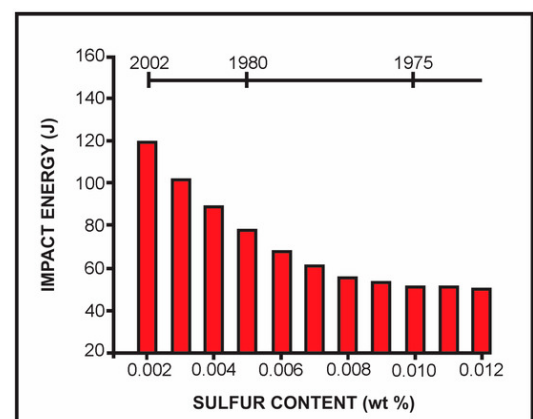

Fig. 8. The effect of sulfur content on the impact strength of pipes [53]

(*IDQ*) methods (Figure 9). The benefits of higher cooling rates and lower coiling temperatures were used to achieve higher strength later with lower carbon steels.

Numerous studies carried out during the period 1956–1980 related to the production of microalloyed steel and hot rolling indicated that the latter was to become the main route of steel production. In a short time this led to the introduction of computer control and modeling to produce small, less than 10 μm, uniformly distributed ferrite grains (Figure 9).
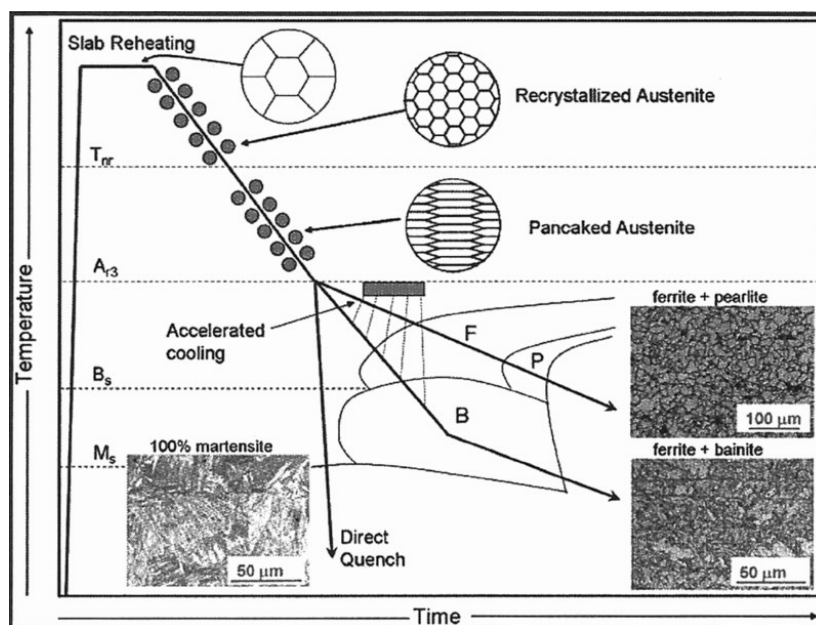

Fig. 9. Schematic diagram of thermomechanically controlled processing (*TMCP*) and microstructures resulting from this process [14]
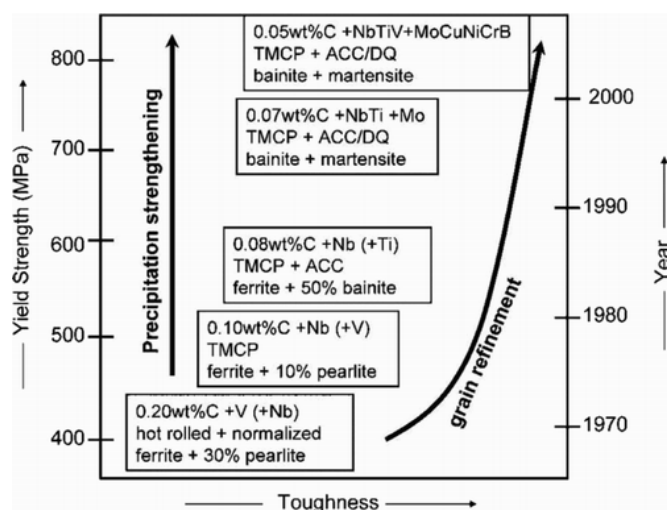

Fig. 10. Development of pipe steels using the example of *HSLA* steel research:

TMCP – thermomechanical controlled rolling; *ACC* – accelerated cooling; *DQ*: direct quenching [14]

Figure 10 schematically shows how the microstructure and properties of steels have changed over time due to advances in steel development and processing. The chemical composition of the steel and the temperature at which rolling is carried out are critical factors affecting the microstructure, phase composition and texture development of steels.

The thermomechanical control process is an effective method that combines controlled rolling and controlled cooling technology to obtain superior comprehensive mechanical properties by controlling the formation of microstructure during deformation [1–3, 12–22]. Due to the low carbon content and micro-alloying combined with various thermomechanical controlled rolling (*TMCR*) conditions, the microstructure of high-strength pipe steel generally contains various microstructural components such as polygonal ferrite (*PF*), quasi-polygonal ferrite (*QF*), acicular ferrite (*AF*), bainite and martensitic-austenitic (*MA*) components, forming a complex mixed microstructure with different characteristics. The addition of micro-alloying elements such as *Mn*, *Mo*, *Cr*, *Ni*, *V*, *Nb* and *Ti* can help obtain ideal microstructure and mechanical properties [45, 46, 52–56].

Thermo-mechanical treatment

The importance of obtaining a fine grain size in terms of increasing both strength and toughness is evident from the original work of *Hall* [81] and *Petch* [82], who experimentally showed for a number of polycrystalline metals that the yield stress $\sigma_{0.2}$ at constant strain is associated with grain diameter d by a certain ratio [83].

Thermomechanical treatment of steel can be divided into three large groups depending on whether the deformation process occurs before, during or after the phase transformation. Processes used include high temperature thermomechanical treatment (*HTMT*), controlled rolling and low temperature thermomechanical treatment (*LTMT*).

When rolling plain carbon-manganese (*C-Mn*) steel sheet (Figure 11), the grain size can be reduced from 10 µm to 5 µm when the sheet is controlled by the degree of deformation and accelerated cooling. This reduction in grain size increases the yield strength of the steel by approximately 80 MPa according to the well-known *Hall-Petch* relationship [81–83].
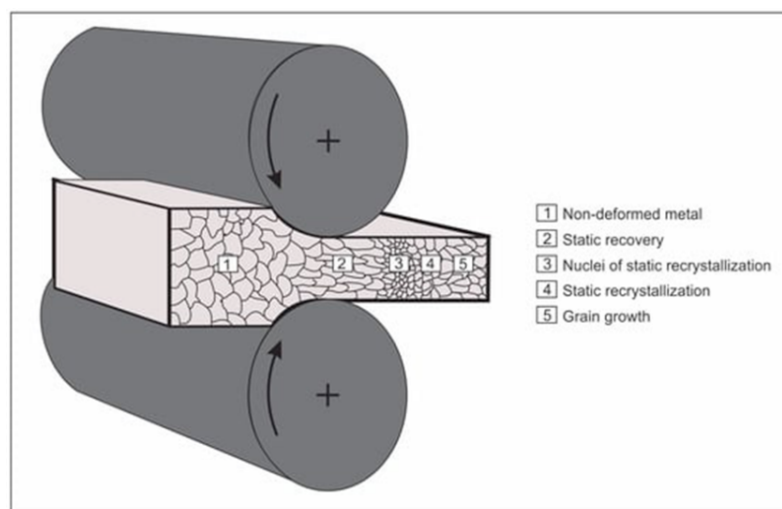

Fig. 11. Schematic diagram of grain refinement in steels during deformation

Controlled rolling is a means by which the properties of steels can be improved to levels equivalent to those of higher alloy or heat treated steels. Controlled rolling consists of three stages: (*a*) deformation in the recrystallization region at high temperatures, (*b*) deformation in the non-recrystallization region, and (*c*) deformation in the austenite-ferritic region. The significance of deformation in the non-recrystallization region lies in the division of austenite grains into several blocks as a result of the introduction of deformation bands into the grains. Deformation in the austenitic-ferritic region gives a mixed structure consisting of equiaxed grains and subgrains. The fundamental difference between conventionally hot-rolled and controlled-rolled steels is that ferrite nucleation occurs exclusively at the austenite grain boundaries in the former, while in the latter it occurs within the grains as well as at the grain boundaries, resulting in finer structures.

Conventional controlled rolling aims to produce flattened austenite grains through plastic deformation, resulting in an increase in nucleation sites for the transformation of austenite to ferrite. This process then results in the formation of fine ferrite grains measuring approximately 5 to 8 µm in size. Traditional controlled rolling usually involves high heating temperatures to achieve complete transition of micro-alloying elements, i.e. *Nb* and *V*, into solid solution.

During the rolling process [14, 51–56, 84–98], which occurs below zero recrystallization temperature, deformation precipitation of *Nb*(*C,N*) occurs, causing complete suppression of recrystallization between each pass. The small size of the austenite grain leads to the refinement of ferrite grains. When deforming in the non-recrystallized temperature range of the austenite phase (below the non-recrystallization tempera-

ture T_{nr} [53]), austenite grains are sintered and deformation structures are introduced inside the grains [53, 84–98]. Deformation at this stage significantly increases the rate of nucleation at the boundaries of austenite grains and within austenite grains. This intragranular nucleation of ferrite is one of the most important
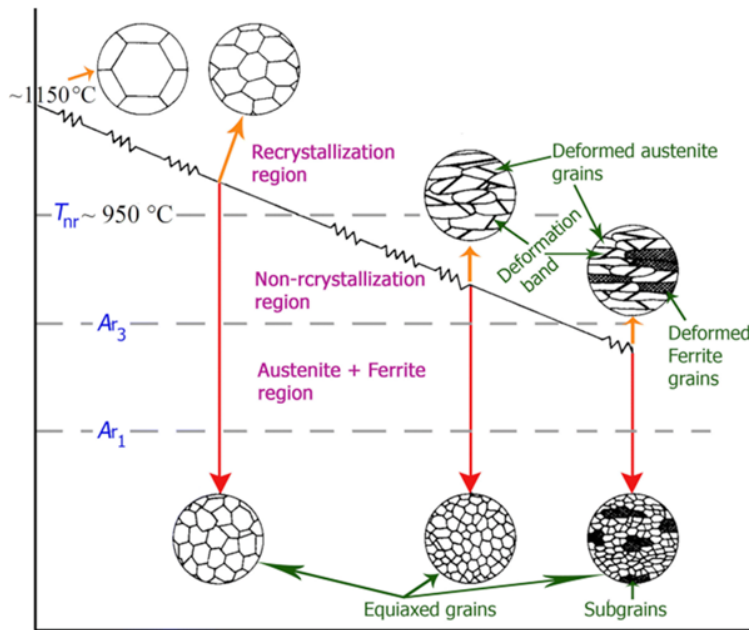

Fig. 12. Schematic diagram of grain refinement in steels during thermomechanical processing [98]

aspects of controlled rolling. Microalloying elements such as niobium and titanium can increase the austenite recrystallization stopping temperature, thereby facilitating the use of this route. Deformation in the intercritical region leads to further strengthening of austenite and the formation of a substructure in ferrite. Accelerated cooling in the austenite-to-ferrite range reduces the ferrite grain size and increases both the strength and toughness of the steel. These routes are shown schematically in Figure 12.

The synergistic effect from the interaction of the processes of austenite recrystallization and deformation precipitation of microalloying elements is one of the important technological issues [84–99]. In order to study the above processes, recrystallization-precipitation-temperature-time (*RPTT*) diagrams have been developed based on recrystallization and precipitation curves [53], where an example of such a diagram is shown in Figure 13. Below the precipitate solubility temperature (T_0), three interaction modes are possible [53 , 86].

In *mode 1*, recrystallization is completed (based on the curves for the beginning of recrystallization R_s and the end of recrystallization R_f) before particle precipitation begins, and thus the stop of recrystallization is not achieved. Accordingly, recrystallized austenite eventually precipitates particles along the *Ps* curve.

In *mode 2*, particle separation begins along the $P^D s$ curve, where the formation of new and powerful nucleation centers occurs due to plastic deformation.

In *mode 3*, particle precipitation occurs before recrystallization, and now both the beginning and the end of recrystallization are stopped [86].

There are different groups of recrystallization processes (see Figures 14–16), many of it are interconnected and the boundaries between them are often unclear. The term recrystallization is commonly used to describe the replacement of the strain microstructure by new grains during annealing; this is called *static recrystallization* (*SRX*) [100]. *SRX* occurs when strain-hardened metals are heated above about half the melting temperature, i.e., 0.5 $T_{melting}$. The temperature at which this can be achieved is usually called the T_{REX} recrystallization temperature. The latter depends on the type of lattice, the concentration of alloying elements and the size

Fig. 13. Schematic representation of the *RPTT* diagram [86]

distribution of secondary phases [100]. During annealing, the microstructure is characterized by a mixture of an increasing number of recrystallized grains and a decreasing number of deformed grains. This process is sometimes called discontinuous static recrystallization (*dSRX*) [100, 101].
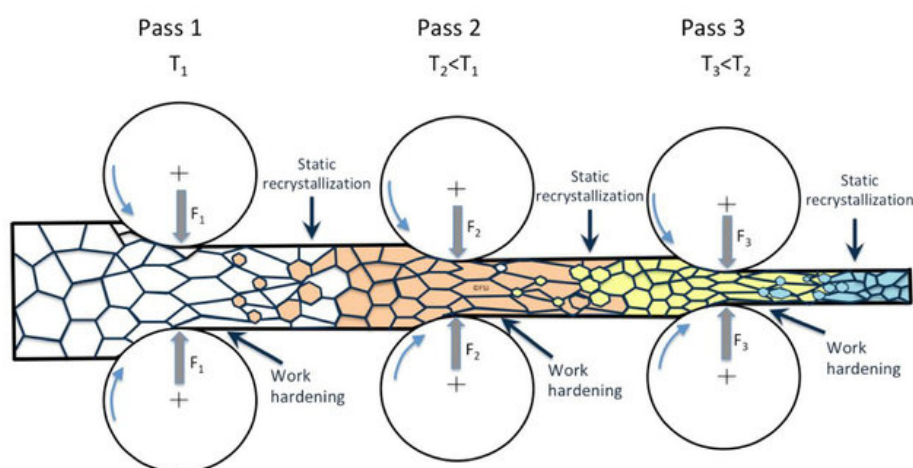
Fig. 14. Schematic representation of the evolution of the microstructure during
rolling controlled by recrystallization [97]:
T – temperature; *F* – rolling force

Fig. 15. Schematic representation of the evolution of the microstructure
during a conventional controlled rolling process [97]:
T – temperature; *F* – rolling force
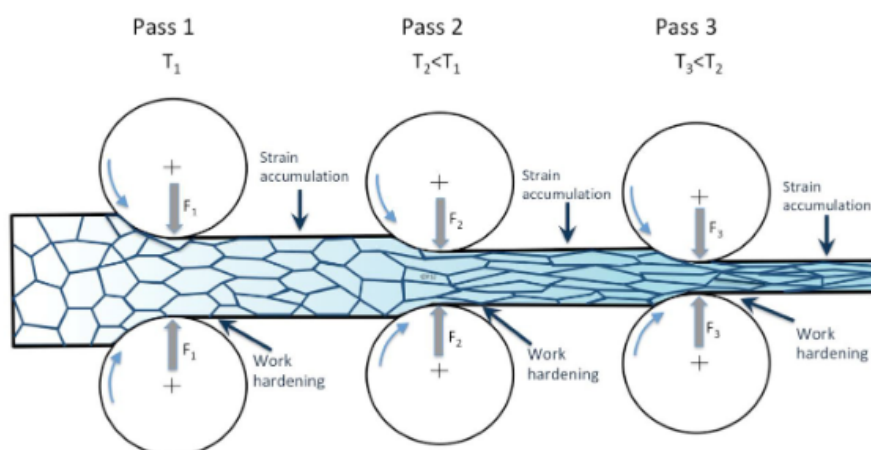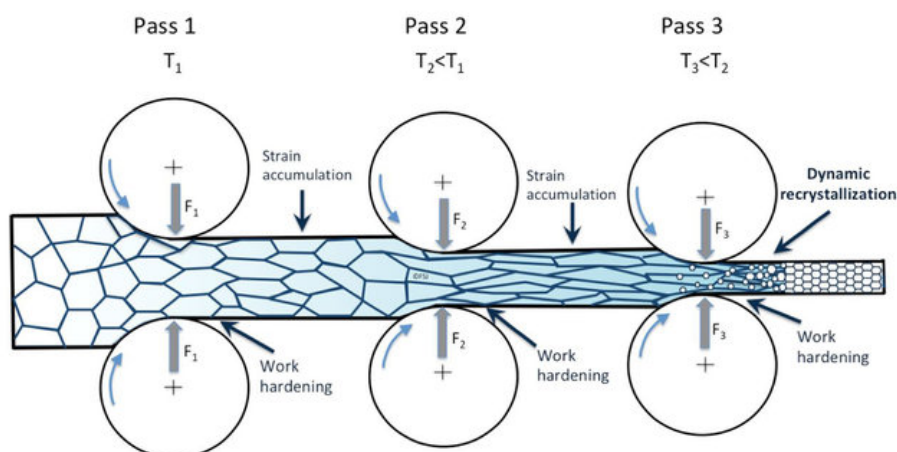

Fig. 16. Schematic representation of the evolution of the microstructure during
the usual process of dynamic recrystallization under controlled rolling [97]:
T – temperature; *F* – rolling force

In contrast, normal dynamic recrystallization (i.e. *dDRX*) occurs during deformation as long as the temperature is above about 0.5 $T_{melting}$. New grains appear during nucleation deformation and then completely replace the original microstructure at high deformations (Figure 16). As in the case of *SRX* (Figure 14), there is a gradual transformation of subgrains, formed mainly near the grain boundaries. These dynamic processes, which include a nucleation step, are similar to those that occur during *dSRX* and are sometimes referred to as discontinuous dynamic recrystallization (*dDRX*) [101]. It has been established that the dynamic mechanism differs significantly from the mechanism of static recrystallization. The latter leads to the formation of a homogeneous and dislocation-free grain structure. As a result, *dDRX* grains initially have wavy boundaries and contain dislocation substructures that vary from grain to grain [101]. Even after *dDRX* has fully developed, regions containing substructures continue to be present, unlike materials that have undergone *dSRX*.

Dynamic recrystallization controlled rolling involves initiating dynamic recrystallization in one or more passes during the rolling process. It is typical for the rolling of wire and rods on continuous rolling lines, as well as the rolling of strips and seamless pipes [97]. This can be achieved by applying large strain in a single pass or by accumulating strain over several separate passes. In both methods, a critical strain is required to initiate dynamic recrystallization. The final grain size of ferrite can reach 1–2μm [1–3, 46, 47, 51–58, 84–99].

The analysis of literature sources shows that the traditional way (until the 1970s) to fine-grained structural steels with ferrite-perlite structure (*FP*) consisted in the inclusion of grain-refining elements such as aluminum, and then in the normalization of materials at a temperature of about 920 °C after rolling [1–3, 12–22, 45, 46, 52–56].

The author [14, 55] notes that "when steel treated with niobium was normalized to improve impact properties, the strength advantage was lost." Thus, there was a need for an alternative route to fine grain structural steel sheet.

One of the problems associated with high-strength low-alloy (*HSLA*) steels is the complex interaction of its strengthening mechanisms, which makes it difficult to optimize its manufacturing parameters. The chemical composition of the steel preliminarily determines the constituent phases in the microstructure. The matrix component can be austenitic, ferritic, pearlitic, martensitic or bainitic, which is a critical factor in the grain refinement process due to differences in crystal structure, microstructural configuration, defects, stacking fault energy (*SFE*), deformation and annealing. On the other hand, the *TMCR* temperature promotes the release of microalloying elements [48, 49, 50, 51, 52].

In 2016, the authors of [93, 94] reported on high-strength low-alloy (*HSLA*) steel. At a *TMCR* temperature of 579 °C, the reported yield strength (*YS*) was in the range of 701–728 MPa, the tensile strength was 996–997 MPa, and the elongation was 21–23 %. At *TMCR* temperature of 621 °C, the yield strength, tensile strength and elongation were in the range of 749–821 MPa, 821–876 MPa and 19–25%, respectively.

Since the mid-1960s, steel mills began to produce fine-grained structural steels by reducing the final rolling temperature [85–105]. The basic idea was to improve the strength and toughness characteristics of structural steels by grain refinement. Compared to conventional hot rolling at high rolling temperatures, new steels were rolled at a lower final rolling temperature. It has been established that repeated recrystallization of austenitic structures leads to a decrease in grain size, but there is a limit that is difficult to overcome. Deformation at temperatures at which recrystallization does not occur was effective in deforming austenite, which had a dense population of slip planes, a high dislocation density, and a high intrinsic energy, which provided a high nucleation density for the austenite transformation products. Initially, ferrite-pearlite microstructures were primarily considered, and then the role of rapid cooling became an additional opportunity to increase the level of strength.

Higher cooling rates or greater undercooling increase the driving force, and with a lower diffusion coefficient, finer microstructures such as bainite and martensite can be achieved. A comparison of the contribution of the hardening mechanism in industrial hot-rolled structural steel with that in fine-grained structural steel is shown in Figure 17 [103].
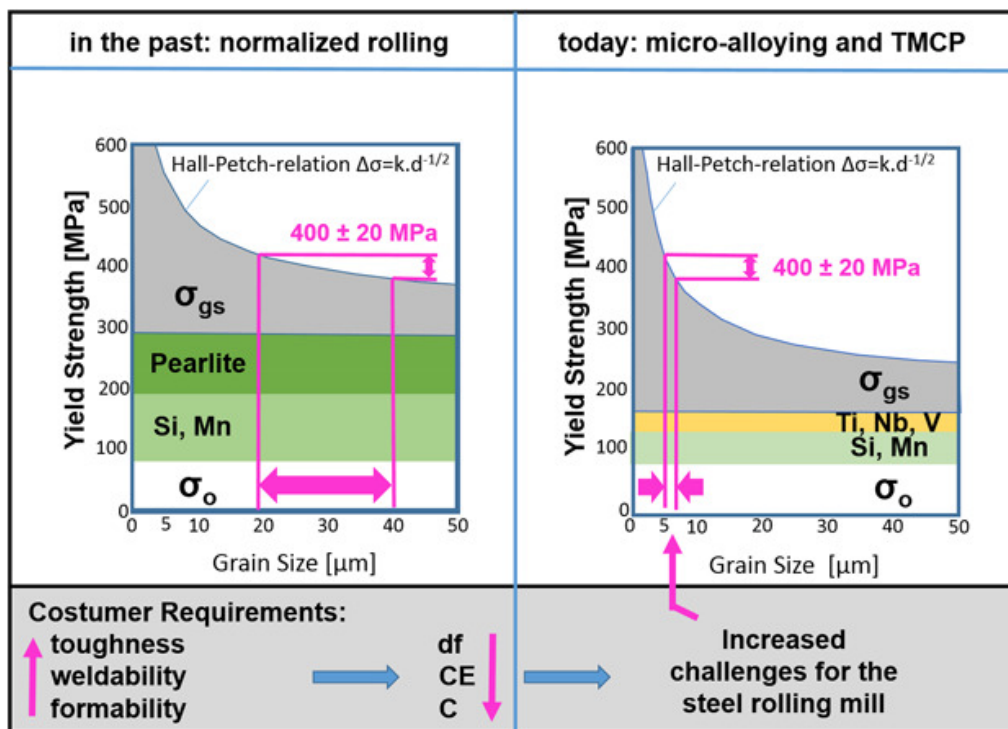
Fig. 17. Typical difference in the contributions of hardening mechanisms in the case of recrystallization controlled rolling at a high temperature of finishing rolling and thermomechanical controlled rolling at a finishing temperature of about 900 °C [103]

From the analysis of the literature above, it is clear that by adding microalloying elements such as *Ti*, *Nb* and *V*, grain growth, recrystallization and particle precipitation kinetics can be controlled. *TiN* is thermodynamically quite stable and helps prevent grain growth at high temperatures, especially in the heat-affected zone of welded joints.

Nb is less stable compared to *Ti* and forms carbon nitrides *Nb*(*C*,*N*) at approximately 900 °C, which nucleate under the influence of deformation and slow down the recrystallization of deformed austenite [14–16]. After rolling, the deformed austenite transforms into ferrite and pearlite, and *V*(*C*,*N*) is released in the ferrite phase, which also gives some increase in strength. The temperature-time dynamics changed from conventional high-temperature rolling to recrystallization-controlled rolling to thermomechanical controlled rolling or *TM* rolling plus rapid cooling after rolling, as shown in Figure 18. As shown, *TMCR* consists of two successive stages: controlled rolling and the subsequent process accelerated cooling. During finish rolling in a hot strip mill, the austenite grains are pulled into a pancake-shaped shape with a high dislocation density.

Until the 1980s, air, air/water mist, oil or water quenching were selected to achieve proper mechanical properties based on *CCT* charts and sheet thickness. Cooling has now become much more flexible, allowing new strategies with new resulting microstructures, as shown in Figure 19 [103].

For plates, accelerated cooling (*ACC*), direct quenching (*DQ*) and direct quenching and self-tempering (*DQST*) were introduced [103].

To provide high cooling rates with stringent requirements for uniformity and controllability, equipment manufacturers were forced to develop advanced cooling systems. Comprehensive control of residual stresses and deformations, increasing the heat transfer coefficient took a lot of time and is currently still the subject of research and development. In other cases, quenching and tempering was replaced by quenching, rapid cooling, isothermal exposure in the field of the bainite phase, and many other possibilities [103]. New cooling strategies have also led to the emergence of new steel grades such as dual-phase (*DP*), complex-phase (*CP*) and transition ductility (*TRIP*) steels.
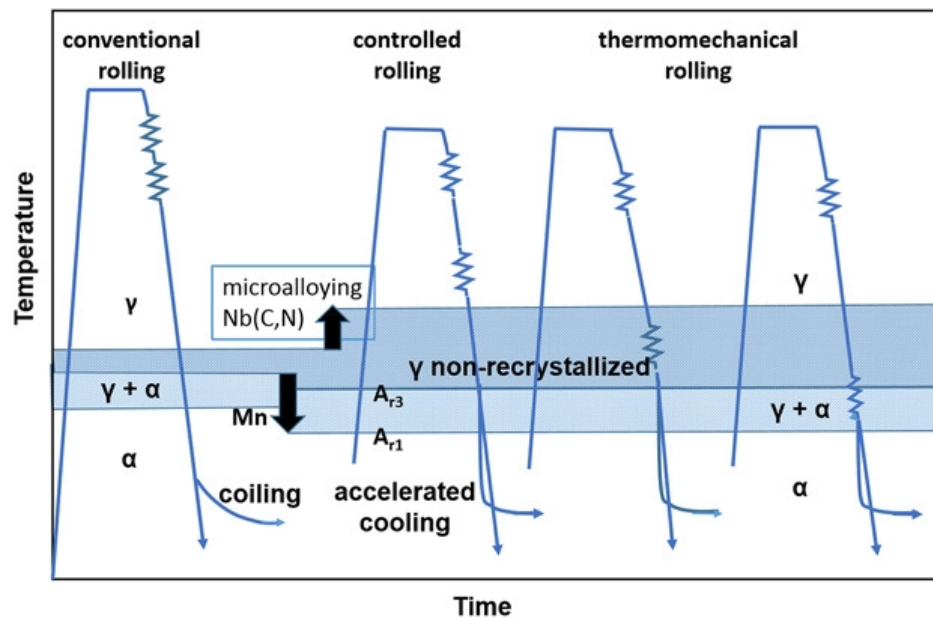
Fig. 18. Rolling strategies from conventional rolling to
thermomechanical rolling with accelerated cooling [103]
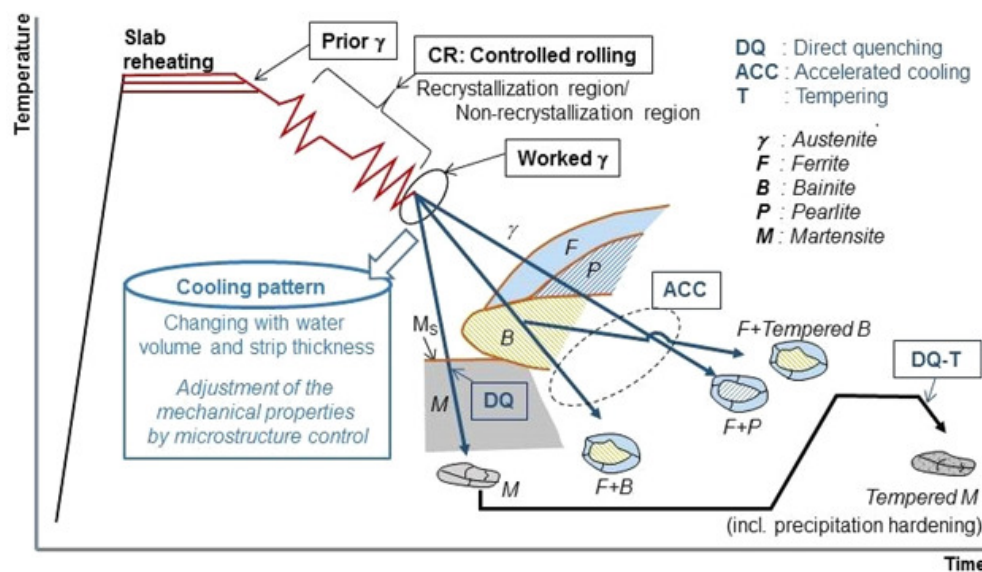
Fig. 19. Scheme of thermomechanical rolling and cooling of high-strength sheets or
strips [103]

High-speed deformation occurs immediately below the γ→α transformation temperature. Due to the heat generated by the deformation, the ferrite turns into austenite for a while before changing back to ferrite.

High ferrite stress is used to initiate dynamic recovery. However, this approach cannot result in ultra-fine grain size, but ferrite grain size of ~ 3 μm can be achieved. This is due to the fact that further grain refinement in ferrite is very difficult due to the low strain hardening index and higher stacking fault energy of ferrite.

Deformation of coarse-grained austenite beyond the critical strain leads to intragranular nucleation of ferrite within the austenite grains, which leads to significant refinement of the ferrite grains. This mechanism is believed to work by forming a layer of ultra-thin ferrite on the surface of a thin strip.

Conclusion

With 71 years of use in industrial steels, niobium has been proven to be beneficial for several properties such as strength and toughness. During this time, numerous studies have been conducted and papers published showing that both strength and toughness can be improved by higher *Nb* additions.

Currently, analytical techniques such as high-resolution X-ray experiments are used, which can be carried out to accurately measure the volume fraction of *NbC* and the corresponding dissolved *Nb* in steel after reheating conditions, which are difficult to measure using electron microscopy or conventional X-ray diffraction due to the very low volume fraction (about 0.0001–0.0002) of niobium carbide precipitation in the steels studied.

In recent decades, *TMCR* has been the most important development for structural steels and has replaced older grades of steel due to its inherent advantages such as increased strength and toughness combined with better weldability and formability. *TMCR* consists of two main functions: deformation of austenite by controlling recrystallization kinetics and applying a proper cooling strategy to create a microstructure according to technical requirements.

Based on existing *TMCR* microstructural models, the entire rolling and cooling process can be much better controlled, resulting in tighter tolerances and supporting the production of new steel grades with improved performance properties. Integrated built-in models will replace stand-alone models. Real-time calculations of microstructure development and precise sensors help control the entire production process and ensure the highest quality products.

References

1. Efron L.I. *Metallovedenie v «bol'shoi» metallurgii. Trubnye stali* [Metallurgy in "big" metallurgy. Pipe steels]. Moscow, Metallurgizdat Publ., 2012. 696 p. ISBN 978-5-902194-63-7.

2. Matrosov Yu.I., Litvinenko S.A., Golovanenko S.A. *Stal' dlya magistral'nykh truboprovodov* [Steel for main pipelines]. Moscow, Metallurgiya Publ., 1989. 288 p.

3. Shiryaev A.G., Chetverikov S.G., Chikalov S.G., Pyshmintsev I.Yu., Krylov P.V. Tekhnologii proizvodstva stal'nykh besshovnykh trub dlya dobychi trudnoizvlekaemykh uglevodorodov [Manufacturing technologies of steel seamless tubes for production of hard-to-recover hydrocarbons]. *Izvestiya vysshikh uchebnykh zavedenii. Chernaya metallurgiya = Izvestiya. Ferrous Metallurgy*, 2018, vol. 61 (11), pp. 866–875. DOI: 10.17073/0368-0797-2018-11-866-875.

4. API Spec 5CT. *Obsadnye i nasosno-kompressornye truby. Tekhnicheskie usloviya* [API Spec 5CT. Casing and tubing. Specifications]. 9th ed. American Petroleum Institute Publ., 2011. 287 p.

5. ISO 11960. *Petroleum and natural gas industries – Steel pipes for use as casing or tubing for wells*. 4th ed. International Organization for Standardization, 2011. 269 p.

6. DSTU ISO 11960:2020. *Petroleum and natural gas industries – Steel pipes for use as casing and tubing for wells*. Geneva, Switzerland, IOS, 2020.

7. GOST R 53366–2009. *Truby stal'nye, primenyaemye v kachestve obsadnykh ili nasosno-kompressornykh trub dlya skvazhin v neftyanoi i gazovoi promyshlennosti. Obshchie tekhnicheskie usloviya* [State Standard R 53366–2009. Steel pipes for use as casing or tubing for wells in petroleum and natural gas industries. General specifications]. Moscow, Standardinform Publ., 2010. 190 p.

8. STO Gazprom 2-4.1-158–2007. *Tekhnicheskie trebovaniya k obsadnym trubam dlya mestorozhdenii OAO «Gazprom»* [Standard organization STO Gazprom 2-4.1-158–2007. Technical requirements for casing pipes for Gazprom fields]. Moscow, Gazprom Publ., 2007. 23 p.

9. STO Gazprom 2-4.1-228–2008. *Tekhnicheskie trebovaniya k nasosno-kompressornym trubam dlya mestorozhdenii OAO «Gazprom»* [Standard organization STO Gazprom 2-4.1-228–2008. Technical requirements for tubing for OAO Gazprom fields]. Moscow, Gazprom Publ., 2008. 32 p.

10. Davies R.J., Almond S., Ward R.S., Jackson R.B., Adams C., Worrall F., Herringshaw L.G., Gluyas J.G., Whitehead M.A. Oil and gas wells and their integrity: Implications for shale and unconventional resource exploitation. *Marine and Petroleum Geology*, 2014, vol. 56, pp. 239–254. DOI: 10.1016/j.marpetgeo.2014.03.001.

11. Li B., Luo M., Yang Z., Yang F., Liu H., Tang H., Zhang Z., Zhang J. Microstructure evolution of the semi-macro segregation induced banded structure in high strength oil tubes during quenching and tempering treatments. *Materials*, 2019, vol. 12 (20), p. 3310. DOI: 10.3390/ma12203310.

12. Zhang Q., Yuan Q., Xiong Z., Liu M., Xu G. Effects of Q&T parameters on phase transformation, microstructure, precipitation and mechanical properties in an oil casing steel. *Physics of Metals and Metallography*, 2021, vol. 122 (14), pp. 1463–1472. DOI: 10.1134/S0031918X21140180.

13. Heisterkamp F., Hulka K., Matrosov Yu.I., Morozov Y.D., Efron L.I., Stolyarov V.I., Chevskaya O.N. *Niobiisoderzhashchie nizkolegirovannye stali* [Niobium containing low alloy steels]. Moscow, Intermet Engineering Publ., 1999. 94 p.

14. Baker T.N. Microalloyed steels. *Ironmaking & Steelmaking*, 2016, vol. 43 (4), pp. 264–307. DOI: 10.1179/1 743281215Y.0000000063.

15. Baker T.N. Titanium microalloyed steels. *Ironmaking & Steelmaking*, 2019, vol. 46 (1), pp. 1–55. DOI: 10.1 080/03019233.2018.1446496.

16. Pickering F.B. Overview of titanium microalloyed steels. *Titanium technology in microalloyed steels*. Ed. by T.N. Baker. London, The Institute of Materials, 1997, pp. 10–43.

17. Takahashi M. Sheet steel technology for the last 100 years: Progress in sheet steels in hand with the automotive industry. *Tetsu To Hagane*, 2014, vol. 100 (1), pp. 82–93. DOI: 10.2355/tetsutohagane.100.82. (In Japanese).

18. Belato Rosado D., De Waele W., Vanderschueren D., Hertelé S. Latest developments in mechanical properties and metallurgical features of high strength line pipe steels. *International Journal of Sustainable Construction and Design*, 2013, vol. 4 (1). DOI: 10.21825/scad.v4i1.742.

19. Joo M.S., Suh D.W., Bhadeshia H.K.D.H. Mechanical anisotropy in steels for pipelines. *ISIJ International*, 2013, vol. 53 (8), pp. 1305–1314. DOI: 10.2355/isijinternational.53.1305.

20. Godefroid L.B., Candido L.C., Toffolo R.B., Barbosa L.H. Microstructure and mechanical properties of two API steels for iron ore pipelines. *Materials Research*, 2014, vol. 17 (suppl 1), pp. 114–120. DOI: 10.1590/S1516-14392014005000068.

21. Tanaka T. Controlled rolling of steel plate and strip. *International Metals Reviews*, 1981, vol. 26 (1), pp. 185–212. DOI: 10.1179/imr.1981.26.1.185.

22. Wang W., Yan W., Zhu L., Hu P., Shan Y., Yang K. Relation among rolling parameters, microstructures and mechanical properties in an acicular ferrite pipeline steel. *Materials & Design*, 2009, vol. 30 (9), pp. 3436–3443. DOI: 10.1016/j.matdes.2009.03.026.

23. Wang C., Cao W.Q., Han Y., Wang C.Y., Huang C.X., Dong H. Influences of austenization temperature and annealing time on duplex ultrafine microstructure and mechanical properties of medium Mn steel. *Journal of Iron and Steel Research International*, 2015, vol. 22 (1), pp. 42–47. DOI: 10.1016/S1006-706X(15)60007-3.

24. Kim N.J., Thomas G. Effects of morphology on the mechanical behavior of a dual phase Fe/2Si/0.1C steel. *Metallurgical Transactions A*, 1981, vol. 12, pp. 483–489. DOI: 10.1007/BF02648546.

25. Liang X. *The complex phase transformation of austenite in high strength linepipe steels and its influence on the mechanical properties*. Diss. University of Pittsburgh, 2012.

26. Kim Y.M., Kim S.K., Lim Y.J., Kim N.J. Effect of microstructure on the yield ratio and low temperature toughness of linepipe steels. *ISIJ International*, 2002, vol. 42 (12), pp. 1571–1577. DOI: 10.2355/isijinternational.42.1571.

27. Shin S.Y., Hong S., Bae J.-H., Kim K., Lee S. Separation phenomenon occurring during the Charpy impact test of API X80 pipeline steels. *Metallurgical and Materials Transactions A*, 2009, vol. 40, pp. 2333–2349. DOI: 10.1007/s11661-009-9943-9.

28. Yang X.-L., Xu Y.-B., Tan X.-D., Wu D. Relationships among crystallographic texture, fracture behavior and Charpy impact toughness in API X100 pipeline steel. *Materials Science and Engineering: A*, 2015, vol. 641, pp. 96–106. DOI: 10.1016/j.msea.2015.06.029.

29. Shanmugam S., Misra R.D.K., Hartmann J., Jansto S. Microstructure of high strength niobium-containing pipeline steel. *Materials Science and Engineering: A*, 2006, vol. 441 (1–2), pp. 215–229. DOI: 10.1016/j.msea.2006.08.017.

30. Sohn S.S., Han S.Y., Bae J.H., Kim H.S., Lee S. Effects of microstructure and pipe forming strain on yield strength before and after spiral pipe forming of API X70 and X80 linepipe steel sheets. *Materials Science and Engineering: A*, 2013, vol. 573, pp. 18–26. DOI: 10.1016/j.msea.2013.02.050.

31. Han S.Y., Sohn S.S., Shin S., Bae J.H., Kim H.S., Lee S. Effects of microstructure and yield ratio on strain hardening and Bauschinger effect in two API X80 linepipe steels. *Materials Science and Engineering: A*, 2012, vol. 551, pp. 192–199. DOI: 10.1016/j.msea.2012.05.007.

32. Bott I.S., Souza L.F.G. De, Teixeira J.C.G., Rios P.R. High-strength steel development for pipelines: a Brazilian perspective. *Metallurgical and Materials Transactions A*, 2005, vol. 36, pp. 443–454. DOI: 10.1007/s11661-005-0315-9.

33. Grimpe F., Meuser H., Gerdemann F., Muthmann E. Improvement of mechanical properties of heavy plates for high strength pipeline application i.e. in Arctic regions. *2nd International Conference on Super-High Strength Steels*, 17–20 October 2010. Associazione Italiana di Metallurgia (AIM), 2010, pp. 1–13.

34. Hillenbrand H.-G., Kalwa C., Schröder J., Kassel C. Challenges to a pipe manufacturer driven by worldwide pipe projects. *18th Joint Technical Meeting on Pipeline Research*, 2011, vol. 13, pp. 1–12.

35. Nonn A., Kalwa C. Modelling of damage behaviour of high strength pipeline steel. *18th European Conference on Fracture*, Dresden, 2010, pp. 1–8.

36. Peiganovich N.V. Vypusk neftegazoprovodnykh trub s povyshennoi ekspluatatsionnoi nadezhnost'yu [Production of oil-and-gas pipeline tubes and casings with increased operate reliability]. *Metallurg = Metallurgist*, 2007, № 12, pp. 51–55. (In Russian).

37. Shabalov I.P., Morozov Yu.D., Efron L.I. *Stali dlya trub i stroitel'nykh konstruktsii s povyshennymi ekspluatatsionnymi svoistvami* [Steels for pipes and building structures with increased performance properties]. Moscow, Metallurgizdat Publ., 2003. 520 p.

38. Mentyukov K.Yu. *Vliyanie termomekhanicheskoi obrabotki pri proizvodstve prokata i trubnogo peredela na strukturu i mekhanicheskie svoistva nizkolegirovannykh stalei dlya trub bol'shogo diametra.* Diss. dokt. tekhn. nauk [The influence of thermomechanical processing in the production of rolled products and pipe processing on the structure and mechanical properties of low-alloy steels for large-diameter pipes. Dr. eng. sci. diss.]. Moscow, 2017. 122 p.

39. Patel D., Thakar V., Pandian S., Shah M., Sircar A. A review on casing while drilling technology for oil and gas production with well control model and economical analysis. *Petroleum*, 2019, vol. 5 (1), pp. 1–12. DOI: 10.1016/j.petlm.2018.12.003.

40. Fontenot K.R., Lesso B., Strickler R.D., Warren T. Using casing to drill directional wells. *Oilfield Review*, 2005, vol. 17 (2), pp. 44–61.

41. Hahn D., Van Gestel W., Fröhlich N., Stewart G. Simultaneous drill and case technology-case histories, status and options for further development. *IADC/SPE Drilling Conference*, New Orleans, Louisiana, February 2000. DOI: 10.2118/59126-MS.

42. Radwan A., Karimi M. Feasibility study of casing drilling application in hpht environments: A review of challenges, benefits, and limitations. *SPE/IADC Middle East Drilling Technology Conference and Exhibition*, Muscat, Oman, October 2011. DOI: 10.2118/148433-MS.

43. Verhoeven J.D. A review of microsegregation induced banding phenomena in steels. *Journal of Materials Engineering and Performance*, 2000, vol. 9 (3), pp. 286–296. DOI: 10.1361/105994900770345935.

44. Morrison W.B. Microalloy steels – the beginning. *Materials Science and Technology*, 2009, vol. 25 (9), pp. 1066–1073. DOI: 10.1179/174328409X453299.

45. Morrison W.B. Influence of small niobium additions on properties of carbon-manganese steels. *Journal of the Iron and Steel Institute*, 1963, vol. 201 (4), pp. 317–325.

46. Webel I., Mohrbacher H., Detemple E., Britz D., Mücklich F. Quantitative analysis of mixed niobium-titanium carbonitride solubility in HSLA steels based on atom probe tomography and electrical resistivity measurements. *Journal of Materials Research and Technology*, 2022, vol. 18, pp. 2048–2063. DOI: 10.1016/j.jmrt.2022.03.098.

47. Webel J., Herges A., Britz D., Detemple E., Flaxa V., Mohrbacher H., Mücklich F. Tracing microalloy precipitation in Nb-Ti HSLA steel during austenite conditioning. *Metals*, 2020, vol. 10, p. 243. DOI: 10.3390/met10020243.

48. Cuddy L.J. The effect of microalloy concentration on the recrystallization of austenite during hot deformation. *Thermomechanical Processing of Microalloyed Austenite*, Warrendale, PA, The Metallurgical Society / AIME, 1982, pp. 129–140. ISBN 0-89520-398-7.

49. DeArdo A.J., Hua M.J., Cho K.G., Garcia C.I. On strength of microalloyed steels: an interpretive review. *Materials Science and Technology*, 2009, vol. 25 (9), pp. 1074–1082. DOI: 10.1179/174328409X455233.

50. Vervynckt S., Verbeken K., Lopez B., Jonas J.J. Modern HSLA steels and role of non-recrystallisation temperature. *International Materials Reviews*, 2012, vol. 57 (4), pp. 187–207. DOI: 10.1179/1743280411y.0000000013.

51. DeArdo A.J. Niobium in modern steels. *International Materials Review*, 2003, vol. 48 (6), pp. 371–402. DOI: 10.1179/095066003225008833.

52. Gladman T. *The physical metallurgy of microalloyed steels*. Institute of Materials Publ., 1997. 363 p.

53. Xie K.Y., Zheng T., Cairney J.M., Kaul H., Williams J.G., Barbaro F., Killmore C.R., Ringer S.P. Strengthening from Nb-rich clusters in a Nb-microalloyed steel. *Scripta Materialia*, 2012, vol. 66 (9), pp. 710–713. DOI: 10.1016/j.scriptamat.2012.01.029.

54. Soto R., Saikaly W., Bano X., Issartel C., Rigaut G., Charai A. Statistical and theoretical analysis of precipitates in dual-phase steels microalloyed with titanium and their effect on mechanical properties. *Acta Materialia*, 1999, vol. 47 (12), pp. 3475–3481. DOI: 10.1016/S1359-6454(99)00190-1.

55. Zhang L., Kannengiesser T. Austenite grain growth and microstructure control in simulated heat affected zones of microalloyed HSLA steel. *Materials Science and Engineering: A*, 2014, vol. 613, pp. 326–335. DOI: 10.1016/j.msea.2014.06.106.

56. Gu Y., Tian P., Wang X., Han X.-l., Liao B., Xiao F.-r. Non-isothermal prior austenite grain growth of a high-Nb X100 pipeline steel during a simulated welding heat cycle process. *Materials and Design*, 2016, vol. 89, pp. 589–596. DOI: 10.1016/j.matdes.2015.09.039.

57. Kojima A., Yoshii K.-I., Hada T., Saeki O., Ichikawa K., Yoshida Y., Shimura Y., Azuma K. Development of high HAZ toughness steel plates for box columns with high heat input welding. *Nippon Steel Technical Report*, 2004, no. 90, pp. 39–44.

58. Chen Y., Zhang D., Liu Y., Li H., Xu D. Effect of dissolution and precipitation of Nb on the formation of acicular ferrite/bainite ferrite in low-carbon HSLA steels. *Materials Characterization*, 2013, vol. 84, pp. 232–239. DOI: 10.1016/j.matchar.2013.08.005.

59. Karjalainen L.P., Maccagno T.M., Jonas J.J. Softening and flow stress behaviour of Nb microalloyed steels during hot rolling simulation. *ISIJ International*, 1995, vol. 35 (12), pp. 1523–1531. DOI: 10.2355/isijinternational.35.1523.

60. Hansen S.S., Sande J.B.V., Cohen M. Niobium carbonitride precipitation and austenite recrystallization in hot-rolled microalloyed steels. *Metallurgical Transactions A*, 1980, vol. 11, pp. 387–402. DOI: 10.1007/BF02654563.

61. Hu J., Du L.X., Xie H., Gao X.H., Misra R.D.K. Microstructure and mechanical properties of TMCP heavy plate microalloyed steel. *Materials Science and Engineering: A*, 2014, vol. 607, pp. 122–131. DOI: 10.1016/j.msea.2014.03.133.

62. Hu J., Du L.X., Wang J.J., Xie H., Gao C.R., Misra R.D.K. Structure-mechanical property relationship in low carbon microalloyed steel plate processed using controlled rolling and two-stage continuous cooling. *Materials Science and Engineering: A*, 2013, vol. 585, pp. 197–204. DOI: 10.1016/j.msea.2013.07.071.

63. Byun J., Shim J., Cho Y.W., Lee D.N. Non-metallic inclusion and intragranular nucleation of ferrite in Ti-killed C–Mn steel. *Acta Materialia*, 2003, vol. 51 (6), pp. 1593–1606. DOI: 10.1016/S1359-6454(02)00560-8.

64. Miyamoto G., Shinyoshi T., Yamaguchi J., Furuhara T., Maki T., Uemori R. Crystallography of intragranular ferrite formed on (MnS + V(C, N)) complex precipitate in austenite. *Scripta Materialia*, 2003, vol. 48 (4), pp. 371–377. DOI: 10.1016/S1359-6462(02)00451-7.

65. Capdevila C., García-Mateo C., Chao J., Caballero F.G. Effect of V and N precipitation on acicular ferrite formation in sulfur-lean vanadium steels. *Metallurgical and Materials Transactions A*, 2009, vol. 40 (3), pp. 522–538. DOI: 10.1007/s11661-008-9730-z.

66. Babu S.S., Bhadeshia H.K.D.H. Mechanism of the transition from bainite to acicular ferrite. *Materials Transactions, JIM*, 1991, vol. 32 (8), pp. 679–688. DOI: 10.2320/matertrans1989.32.679.

67. Madariaga I., Gutiérrez I., García-de Andrés C., Capdevila C. Acicular ferrite formation in a medium carbon steel with a two stage continuous cooling. *Scripta Materialia*, 1999, vol. 41 (3), pp. 229–235. DOI: 10.1016/S1359-6462(99)00149-9.

68. Aminorroaya Yamini S. Influence of microalloying elements (Ti, Nb) and nitrogen concentrations on precipitation of pipeline steels – A thermodynamic approach. *Engineering Reports*, 2021, vol. 3 (7), p. e12337. DOI: 10.1002/eng2.12337.

69. Zhuo X., Wang X., Wang W., Lee H.G. Nature of large (Ti, Nb)(C, N) particles precipitated during the solidification of Ti, Nb HSLA steel. *Journal of University of Science and Technology Beijing, Mineral, Metallurgy, Material*, 2007, vol. 14 (2), pp. 112–117. DOI: 10.1016/S1005-8850(07)60023-1.

70. Den Boer A.W., Malakhov D.V. Critical role of carbon during production of ferroniobium alloy additions. *Canadian Metallurgical Quarterly*, 2014, vol. 53 (4), pp. 423–431. DOI: 10.1179/1879139514Y.0000000134.

71. Abraham S., Bodnar R., Lonnqvist J., Hagstrom J., Rydgren E. The mechanism for coarse Nb-rich particle formation in steel. *Metallurgical and Materials Transactions A*, 2021, vol. 52, pp. 3727–3749. DOI: 10.1007/s11661-021-06324-3.

72. Uranga P., Isasti N., Jorge-Badiola D., Taheri M.L. Microstructural features controlling mechanical properties in Nb-Mo microalloyed steels. Part I: Yield strength. *Metallurgical and Materials Transactions A*, 2014, vol. 45, pp. 4960–4971. DOI: 10.1007/s11661-014-2450-7.

73. Suzuki S., Kuroki K., Kobayashi H., Takahashi N. Sn segregation at grain boundary and interface between MnS and matrix in Fe-3 mass% Si alloys doped with tin. *Materials Transactions, JIM*, 1992, vol. 33 (11), pp. 1068–1076. DOI: 10.2320/matertrans1989.33.1068.

74. Tsunekage N., Tsubakino H. Effects of sulfur content and sulfide-forming elements addition on impact properties of ferrite-pearlitic microalloyed steels. *ISIJ International*, 2001, vol. 41 (5), pp. 498–505. DOI: 10.2355/isijinternational.41.498.

75. Phillips R., Chapman J.A. Influence of finish rolling temperature on mechanical properties of some commercial steels rolled to 13/16 in. diameter bars. *Journal of the Iron and Steel Institute*, 1966, vol. 204, pp. 615–622.

76. Hiroyoshi M., Osuka T., Kozasu I., Tsukada K. Optimization of metallurgical factors for production of high strength, high toughness steel plate by controlled rolling. *Transactions of the Iron and Steel Institute of Japan*, 1972, vol. 12, pp. 435–443.

77. Hall E.O. The deformation and ageing of mild steel: III discussion of results. *Proceedings of the Physical Society. Section B*, 1951, vol. 64 (9), p. 747. DOI: 10.1088/0370-1301/64/9/303.

78. Petch N.J. The cleavage strength of polycrystals. *Journal of the Iron and Steel Institute*, 1953, vol. 174, pp. 25–28.

79. Armstrong R., Codd I., Douthwaite R.M., Petch N.J. The plastic deformation of polycrystalline aggregates. *The Philosophical Magazine: A Journal of Theoretical Experimental and Applied Physics*, 1962, vol. 7 (73), pp. 45–58. DOI: 10.1080/14786436208201857.

80. Hoogendoorn T.M., Spanraft M.J. Quantifying the effect of microalloy elements on structures during processing. *Proceedings. Microalloying '75*, Washington, 1975, pp. 75–89.

81. Villalobos J.C., Del-Pozo A., Campillo B., Mayen J., Serna S. Microalloyed steels through history until 2018: review of chemical composition, processing and hydrogen service. *Metals*, 2018, vol. 8 (5), p. 351. DOI: 10.3390/met8050351.

82. Palmiere E.J., Garcia C.I., DeArdo A.J. Compositional and microstructural changes which attend reheating and grain coarsening in steels containing niobium. *Metallurgical and Materials Transactions A*, 1994, vol. 25, pp. 277–286. DOI: 10.1007/BF02647973.

83. Gauthier G., LeBon A.B. Discussion: on the recrystallization of austenite. *Proceedings. Microalloying '75*, Washington, 1975, pp. 1–3.

84. Kozasu I., Ouchi C., Sampei T., Okita T. Hot rolling as a high-temperature thermo-mechanical process. *Proceedings. Microalloying '75*, Washington, 1975, pp. 120–134.

85. DeArdo A.J. *Microalloyed steels: fifty years of progress – An interpretive review*. Available at: https://www.researchgate.net/publication/304374754_Microalloyed_Steels_Fifty_Years_of_Progress_-_An_Interpretive_Review (accessed 06.08.2024).

86. Guo F., Wang X., Wang J., Misra R.D.K., Shang C. The significance of central segregation of continuously cast billet on banded microstructure and mechanical properties of section steel. *Metals*, 2020, vol. 10, p. 76. DOI: 10.3390/met10010076.

87. Stalheim D.G. The use of high temperature processing (HTP) steel for high strength oil and gas transmission pipeline applications. *Iron & Steel*, 2005, vol. 40 (11), pp. 699–704.

88. Misra D., Jansto S.G. Niobium-based alloy design for structural applications: processing-structure-property paradigm. *HSLA Steels 2015, Microalloying 2015 & Offshore Engineering Steels 2015: conference proceedings*. Hoboken, NJ, USA, John Wiley & Sons, Inc., 2015, pp. 261–266.

89. Challa V.S.A., Zhou W.H., Misra R.D.K., O'Malley R., Jansto S.G. The effect of coiling temperature on the microstructure and mechanical properties of a niobium–titanium microalloyed steel processed via thin slab casting. *Materials Science and Engineering: A*, 2014, vol. 595, pp. 143–153. DOI: 10.1016/j.msea.2013.12.002.

90. Sarmento E.C., Evans J. Effect of strain accumulation and dynamic recrystallisation on the flow stress of HSLA steels during flat rolling. *Proceedings of an International Symposium on Processing, Microstructure, and Properties of HSLA Steels*: *ISS-AIME 1992*, Warrendale, Pennsylvania, 1992, pp. 105–112.

91. Yada H., Matsumura Y., Senuma T. A new thermomechanical heat treatment for grain refining in low carbon steels. *Proceedings of the 1st International Conference on Physical Metallurgy of Thermomechanical Processing of Steels and Other Metals (THERMEC '88)*, Keidanren Kaikan, Tokyo, Japan, 1988, p. 200.

92. Siciliano F., Rodrigues S.F., Aranas Jr C., Jonas J.J. The dynamic transformation of ferrite above Ae3 and the consequences on hot rolling of steels. *Tecnologia em Metalurgia, Materiais e Mineração*, 2020, vol. 17 (2), pp. 90–95. DOI: 10.4322/2176-1523.20202230.

93. Tamura I., Sekine H., Tanaka T. *Thermomechanical processing of high-strength low-alloy steels*. Butterworth-Heinemann, 2013. ISBN 0-408-11034-1.

94. Nasiri Z., Ghaemifar S., Naghizadeh M., Mirzadeh H. Thermal mechanisms of grain refinement in steels: A review. *Metals and Materials International*, 2021, vol. 27, pp. 2078–2094. DOI: 10.1007/s12540-020-00700-1.

95. Sakai T., Belyakov A., Kaibyshev R., Miura H., Jonas J.J. Dynamic and post-dynamic recrystallization under hot, cold and severe plastic deformation conditions. *Progress in Materials Science*, 2014, vol. 60, pp. 130–207. DOI: 10.1016/j.pmatsci.2013.09.002.

96. Huang K.E., Logé R.E. A review of dynamic recrystallization phenomena in metallic materials. *Materials & Design*, 2016, vol. 111 (8), pp. 548–574. DOI: 10.1016/j.matdes.2016.09.012.

97. Sanz L., Pereda B., López B. Effect of thermomechanical treatment and coiling temperature on the strengthening mechanisms of low carbon steels microalloyed with Nb. *Materials Science and Engineering: A*, 2017, vol. 685, pp. 377–390. DOI: 10.1016/j.msea.2017.01.014.

98. Buchmayr B. Thermomechanical Treatment of steels – A real disruptive technology since decades. *Steel Research International*, 2017, vol. 88 (10), p. 1700182. DOI: 10.1002/srin.201700182.

99. Funakawa Y., Shiozaki T., Tomita K., Yamamoto T., Maeda E. Development of high strength hot-rolled sheet steel consisting of ferrite and nanometer-sized carbides. *ISIJ International*, 2004, vol. 44 (11), pp. 1945–1951. DOI: 10.2355/isijinternational.44.1945.

100. Zaitsev A., Arutyunyan N. Low-carbon Ti-Mo microalloyed hot rolled steels: special features of the formation of the structural state and mechanical properties. *Metals*, 2021, vol. 11 (10), p. 1584. DOI: 10.3390/met11101584.

101. Zhao J., Jiang Z. Thermomechanical processing of advanced high strength steels. *Progress in Materials Science*, 2018, vol. 94, pp. 174–242. DOI: 10.1016/j.pmatsci.2018.01.006.

102. Shaposhnikov N.G., Koldaev A.V., Zaitsev A.I., Rodionova I.G., Dyakonov D.L., Arutyunyan N.A. Features of titanium carbide precipitation in low-carbon high-strength steels microalloyed with titanium and molybdenum. *Metallurgist*, 2016, vol. 60 (7–8), pp. 810–816. DOI: 10.1007/s11015-016-0370-z. Translated from *Metallurg*, 2016, no. 8, pp. 49–54.

103. Skeeba V.Yu., Ivancivsky V.V., Martyushev N.V., Lobanov D.V., Vakhrushev N.V., Zhigulev A.K. Numerical simulation of temperature field in steel under action of electron beam heating source. *Key Engineering Materials*, 2016, vol. 712, pp. 105–111. DOI: 10.4028/www.scientific.net/KEM.712.105.

104. Adigamov R.R., Baraboshkin K.A., Yusupov V.S. Study of the phase transition kinetics in the experimental melting of rolled coils of K55 grade strength steel for pipes manufacturing. *Steel in Translation*, 2022, vol. 52 (11), pp. 1098–1105. DOI: 10.3103/S096709122211002X.

105. Adigamov R.R., Baraboshkin K.A., Mishnev P.A., Karlina A.I. Development of rolling procedures for pipes of K55 strength class at the laboratory mill. *CIS Iron and Steel Review*, 2022, Vol. 24, pp. 60–66. DOI: 10.17580/cisisr.2022.02.09.

Conflicts of Interest

The authors declare no conflict of interest.